Research Square

Preprints are preliminary reports that have not undergone peer review.
They should not be considered conclusive, used to inform clinical practice,
or referenced by the media as validated information.

Peripapillary and Conjunctival Optical Coherence Tomography Angiography in Pseudoexfoliation Spectrum: A Two-Domain Analysis

Abbas Mohammadi

abbas19941373@gmail.com

Ahvaz Jundishapur University of Medical Sciencesi

Maryam Hajizadeh

Ahvaz Jundishapur University of Medical Sciencesi

Nasrin Masihpour

Ahvaz Jundishapur University of Medical Sciencesi

Azadeh Samaeili

Ahvaz Jundishapur University of Medical Sciencesi

Fatemeh Naghash Zadeh

Ahvaz Jundishapur University of Medical Sciencesi

Research Article

Keywords: Pseudoexfoliation syndrome, pseudoexfoliation glaucoma, optical coherence tomography angiography, radial peripapillary capillaries, conjunctival OCTA, retinal nerve fiber layer

Posted Date: August 7th, 2026

DOI: https://doi.org/10.21203/rs.3.rs-10305027/v1

License: This work is licensed under a Creative Commons Attribution 4.0 International License.
Read Full License

Additional Declarations: No competing interests reported.

Abstract

Purpose

To evaluate peripapillary structural/vascular and conjunctival OCTA parameters across the pseudoexfoliation (PEX) spectrum, and to determine whether conjunctival OCTA provides a novel microvascular signal beyond conventional peripapillary measurements.

Methods

Cross-sectional analysis of 45 eyes (15 healthy, 15 PEX, 15 PEX glaucoma [PEXG]). Peripapillary variables comprised RNFL thickness and radial peripapillary capillary (RPC) vessel density (VD) in four quadrants. Conjunctival OCTA comprised VD, vessel length density (VLD), and vessel density index (VDI) in nasal/temporal and superficial/deep regions. Group comparisons used Kruskal-Wallis with FDR correction, Holm-adjusted pairwise tests, age/sex-adjusted models, Spearman correlations, and ROC analysis for PEXG vs. non-glaucoma.

Results

Mean RNFL thickness showed the strongest glaucoma-specific signal (90.3 ± 5.3, 82.0 ± 8.1, 61.8 ± 10.7 μm; $p < 0.001$; adjusted $p < 0.001$; $\varepsilon^2=0.67$). Mean RPC VD was lower in PEX and PEXG vs. healthy (57.6 ± 7.1, 45.7 ± 8.9, 43.9 ± 9.1; $p < 0.001$), but age/sex-adjusted effect was not significant ($p = 0.877$). Conjunctival VD, VLD, and VDI were reduced in PEX/PEXG vs. healthy, with no clear PEX-to-PEXG separation. ROC analysis showed excellent discrimination for PEXG using mean RNFL (AUC = 0.96), followed by cup-disc ratio (0.94) and IOP (0.93); conjunctival VDI and VD showed moderate discrimination (AUC = 0.77 and 0.76).

Conclusions

Peripapillary RNFL thinning is the dominant glaucoma-specific biomarker. RPC and conjunctival OCTA reductions are evident by the PEX stage but age-confounded and not independently glaucoma-specific. Conjunctival OCTA represents a novel exploratory anterior-segment microvascular marker in PEX requiring age-matched validation.

INTRODUCTION

Pseudoexfoliation syndrome (PEX) is an age-related systemic extracellular-matrix disorder characterized by abnormal production and progressive accumulation of fibrillar pseudoexfoliative material in ocular and extraocular tissues [1–3]. Within the eye, this material is classically deposited on the anterior lens capsule, pupillary margin, iris, zonules, ciliary body, trabecular meshwork, and vascular structures [3–5].

PEX is clinically important because it represents the most common identifiable cause of secondary open-angle glaucoma worldwide, and pseudoexfoliation glaucoma (PEXG) is often more aggressive than primary open-angle glaucoma, with higher intraocular pressure, greater diurnal fluctuation, poorer pressure control, and faster structural and functional progression [3–5].

Although PEX is frequently recognized by its anterior-segment signs, increasing evidence indicates that it is not limited to the anterior chamber. Histopathological and ultrastructural studies have demonstrated pseudoexfoliative material in conjunctival, orbital, vascular, and other extrabulbar tissues, supporting the concept of PEX as a systemic fibrillopathy with ocular manifestations [6, 7]. This systemic and vascular involvement has important implications. PEX has been associated with altered ocular blood flow, retinal vascular occlusive disease, endothelial dysfunction, and systemic vascular abnormalities [8–10]. Therefore, vascular assessment in PEX may provide information beyond conventional structural glaucoma evaluation.

Optical coherence tomography angiography (OCTA) has expanded glaucoma imaging from structural assessment alone to non-invasive visualization and quantification of retinal and optic nerve head microvasculature [11–13]. In glaucoma, the peripapillary region is particularly relevant because the radial peripapillary capillary (RPC) plexus supplies the retinal nerve fiber layer (RNFL), which contains the retinal ganglion cell axons most directly affected by glaucomatous damage [27, 28]. Reduced peripapillary vessel density has been reported in glaucomatous eyes and often correlates with RNFL thinning and functional severity [11–13].

In the PEX spectrum, OCTA studies have generally shown reduced optic nerve head or peripapillary vessel density in PEXG compared with healthy eyes, and several reports suggest that vascular compromise may also be detectable in PEX eyes before manifest glaucoma [14–19, 23–26]. However, the relationship between microvascular loss and structural damage remains unsettled. Some studies suggest that reduced peripapillary vessel density may precede measurable RNFL loss in PEX [19], whereas others indicate that vascular changes are more prominent in manifest glaucoma and may be closely linked to established structural damage [18]. These divergent findings may reflect differences in age matching, glaucoma severity, OCTA device characteristics, segmentation algorithms, image quality, and analytic strategy.

Most previous OCTA studies in PEX have focused on the posterior segment, particularly the optic nerve head, peripapillary retina, macula, or choroid [14–19, 23–26]. In contrast, the conjunctiva has received comparatively little attention, despite strong biological plausibility. Pseudoexfoliative material has been identified in conjunctival and subconjunctival tissues, and extrabulbar pseudoexfoliative deposition may precede or accompany intraocular disease [6, 7]. The conjunctiva is also directly accessible to non-invasive vascular imaging. Recent advances in anterior-segment and ocular-surface OCTA have enabled quantitative assessment of conjunctival vessel density, vessel length density, and related vascular indices [20–22]. These developments raise the possibility that conjunctival OCTA could capture an anterior-segment or ocular-surface microvascular signal of PEX-related disease burden.

Nevertheless, the clinical value of conjunctival OCTA in the PEX spectrum remains undefined. It is not known whether conjunctival OCTA parameters differentiate healthy eyes from PEX and PEXG, whether they provide information beyond conventional peripapillary RNFL and RPC measurements, or whether they are specific for glaucomatous conversion. This distinction is important. A useful glaucoma biomarker should distinguish PEXG from PEX without glaucoma, whereas a PEX disease-burden biomarker may be abnormal in both PEX and PEXG without necessarily separating the two conditions.

Accordingly, the present study evaluated two anatomically distinct OCT/OCTA domains across the PEX spectrum: a posterior peripapillary domain, including RNFL thickness and RPC vessel density, and an anterior conjunctival domain, including conjunctival vessel density, vessel length density, and vessel density index. We compared these parameters among healthy eyes, PEX eyes without glaucoma, and PEXG eyes; assessed age/sex-adjusted associations; examined relationships with clinical severity markers; and evaluated diagnostic accuracy for PEXG. We hypothesized that peripapillary RNFL thinning would provide the strongest glaucoma-specific signal, whereas RPC and conjunctival OCTA abnormalities would reflect broader microvascular involvement in the PEX spectrum. We further hypothesized that conjunctival OCTA may represent a novel exploratory marker of PEX-related ocular-surface microvascular alteration rather than a stand-alone diagnostic biomarker for PEXG.

MATERIALS AND METHODS

Study Design and Ethical Approval

This cross-sectional observational study was conducted between 2024 and 2025 at the Department of Ophthalmology, Faculty of Medicine, Ahvaz Jundishapur University of Medical Sciences, and the Infectious Ophthalmologic Research Center, Ahvaz, Iran. The study was designed to evaluate posterior peripapillary structural and microvascular parameters together with anterior conjunctival microvascular parameters across the pseudoexfoliation spectrum. The study protocol adhered to the tenets of the Declaration of Helsinki and was approved by the Institutional Review Board/Ethics Committee of Ahvaz Jundishapur University of Medical Sciences (approval number: IR.AJUMS.HGOLESTAN.REC.1404.021). Written informed consent was obtained from all participants before enrollment.

Study Population

A total of 45 eyes were included and divided equally into three groups: healthy control eyes (n = 15), eyes with pseudoexfoliation syndrome without glaucoma (PEX; n = 15), and eyes with pseudoexfoliation glaucoma (PEXG; n = 15). Group allocation was based on clinical examination, intraocular pressure, optic nerve head assessment, retinal nerve fiber layer findings, and visual field information when available.

The healthy control group included eyes without clinical evidence of pseudoexfoliation, glaucoma, or other ocular disease. The PEX group included eyes with clinically visible pseudoexfoliative material but

without glaucomatous optic neuropathy or compatible glaucomatous visual field damage. The PEXG group included eyes with pseudoexfoliative material and evidence of glaucomatous optic neuropathy.

Diagnostic Criteria

Pseudoexfoliation syndrome was diagnosed by the presence of typical pseudoexfoliative material on the anterior lens capsule, pupillary margin, or other anterior segment structures on slit-lamp examination after pharmacologic pupil dilation.

Pseudoexfoliation glaucoma was diagnosed when pseudoexfoliation was accompanied by glaucomatous optic nerve damage, defined by one or more of the following: neuroretinal rim thinning or notching, localized or diffuse RNFL defect, increased cup-disc ratio or cup-disc asymmetry, elevated intraocular pressure, and/or reproducible glaucomatous visual field abnormality when available.

Healthy controls were required to have no pseudoexfoliative material, intraocular pressure less than 22 mmHg, normal optic disc appearance, no glaucomatous RNFL defect, and no history of glaucoma or ocular hypertension.

Inclusion and Exclusion Criteria

Participants were eligible if they were adults able to undergo high-quality OCT and OCTA imaging and if the study eye met criteria for one of the three study groups. Only images with adequate signal strength and without major motion or segmentation artifacts were included.

Eyes were excluded if they had ocular conditions that could affect peripapillary or conjunctival vascular measurements, including diabetic retinopathy, hypertensive retinopathy, retinal vascular occlusion, macular disease, optic neuropathy other than glaucoma, uveitis, active ocular surface inflammation, corneal opacity interfering with image acquisition, or a history of intraocular surgery within the previous 6 months. Eyes with high refractive error greater than ± 4.00 diopters, poor fixation, media opacity preventing reliable imaging, or OCTA images of insufficient quality were also excluded.

Participants with systemic diseases known to significantly affect microvascular parameters, including diabetes mellitus, uncontrolled hypertension, systemic vasculitis, autoimmune inflammatory disease, or current systemic vascular instability, were excluded when such information was available.

Clinical and Ophthalmic Examination

All participants underwent a comprehensive ophthalmic examination by an ophthalmologist. The examination included best-corrected visual acuity, slit-lamp biomicroscopy, intraocular pressure measurement, gonioscopy when available, dilated fundus examination, optic nerve head evaluation, and assessment for pseudoexfoliative material.

Best-corrected visual acuity(BCVA) was recorded and converted to logarithm of the minimum angle of resolution values for analysis. Intraocular pressure was measured using Goldmann applanation tonometry or the standard institutional method. Cup-disc ratio was assessed clinically from dilated optic nerve head examination and/or imaging records. Demographic and clinical variables included age, sex code, best-corrected visual acuity, intraocular pressure, and cup-disc ratio. Because sex labels were coded numerically in the dataset, sex was included as a coded covariate for statistical adjustment without biological interpretation of the code categories.

OCT and OCTA Imaging Protocol

All imaging was performed using the same institutional OCT/OCTA platform and acquisition approach used for anterior segment OCTA imaging in the center. The AngioVue OCTA system (Optovue Inc., Fremont, CA, USA) uses a central wavelength of approximately 840 nm, an A-scan rate of 70,000 scans per second, and the split-spectrum amplitude-decorrelation angiography algorithm for motion-contrast imaging.

Both posterior peripapillary and anterior conjunctival domains were evaluated.

Peripapillary OCT/OCTA Domain

Peripapillary structural and microvascular imaging was performed around the optic nerve head. The structural peripapillary parameter was retinal nerve fiber layer thickness. RNFL thickness was recorded in four quadrants: superior, inferior, nasal, and temporal. Mean RNFL thickness was calculated as the average of the four quadrants.

Radial peripapillary capillary vessel density was measured using OCTA in the peripapillary region. RPC vessel density was recorded in the superior, inferior, nasal, and temporal quadrants. Mean RPC vessel density was calculated as the average of the four sectoral values.

The posterior domain, therefore, consisted of the following primary variables: mean RNFL thickness, RNFL thickness in each quadrant, mean RPC vessel density, and RPC vessel density in each quadrant.

Conjunctival OCTA Domain

Anterior segment OCTA was used to evaluate the bulbar conjunctival microvasculature. Nasal and temporal bulbar conjunctival regions were imaged separately using a 3 × 3 mm scan protocol. Imaging was performed with the participant seated and fixating in the opposite direction to expose the target conjunctival region. Care was taken to avoid excessive eyelid pressure or manipulation that could alter conjunctival blood flow. The conjunctival slab was manually defined from the conjunctival epithelium to approximately 200 μm depth, consistent with the superficial conjunctival segmentation protocol used in the center's prior AS-OCTA work. For each region, superficial and deep conjunctival vascular parameters

were extracted when available. The conjunctival OCTA parameters included vessel density, vessel length density, and vessel density index. These variables were measured in the following regions: nasal superficial, nasal deep, temporal superficial, and temporal deep. Domain-level conjunctival indices were calculated as the mean of the available nasal and temporal superficial/deep values for each parameter. The anterior conjunctival domain therefore, consisted of mean conjunctival vessel density, mean conjunctival vessel length density, mean conjunctival vessel density index, and corresponding sectoral values.

Image Quality Control

All OCT and OCTA images were reviewed before analysis. Images were excluded if they showed poor centration, low signal strength, motion artifact, blink artifact, segmentation error, defocus, shadowing, or unreliable vessel-density output. A minimum signal strength index of 6/10 was required, consistent with the institutional OCTA quality threshold.

Images were reviewed by masked graders who were unaware of the diagnostic group whenever possible. Disagreements regarding image quality or segmentation were resolved by consensus or by review from a senior ophthalmologist. If repeatability data are available for this dataset, inter-grader or intra-grader reproducibility should be reported using the intraclass correlation coefficient.

Statistical Analysis

Data analysis was performed using IBM SPSS Statistics for Windows, version 27 (IBM Corp., Armonk, NY, USA).. Categorical variables were summarized as frequency and percentage. Because of the small sample size and non-normal distribution of several OCT/OCTA variables, primary across-group comparisons were performed using the Kruskal-Wallis test. To control for multiple testing, Benjamini-Hochberg false-discovery-rate correction was applied within clinically relevant domain families. When the overall group effect was significant, post-hoc pairwise comparisons were performed using Holm-adjusted tests. Effect size for Kruskal-Wallis comparisons was reported using epsilon-squared. Percentage change versus healthy controls was calculated for PEX and PEXG groups to facilitate clinical interpretation. Because the healthy group was younger than the PEX and PEXG groups, age/sex-adjusted models were included as a major component of the statistical analysis. For each OCT/OCTA outcome, linear regression models were fitted using the following structure: outcome = diagnostic group + age + sex code. The adjusted p-value for the group term was reported to determine whether the group effect remained significant after accounting for age and sex code. Spearman correlation analysis was used to evaluate monotonic associations between clinical severity markers and OCT/OCTA domain indices. Correlation analyses included BCVA, intraocular pressure, cup-disc ratio, age, mean RNFL thickness, mean RPC vessel density, mean conjunctival VD, mean conjunctival VLD, and mean conjunctival VDI. Diagnostic accuracy for distinguishing PEXG from non-glaucomatous eyes, defined as healthy plus PEX eyes, was assessed using receiver operating characteristic curves. Area under the curve values were calculated with bootstrap 95% confidence intervals. For RNFL, RPC, and conjunctival OCTA parameters, lower values were considered to indicate a higher probability of PEXG. For intraocular pressure and cup-

disc ratio, higher values were considered to indicate a higher probability of PEXG. The Youden index was used to identify exploratory optimal cutoffs, sensitivity, and specificity. A two-sided p-value less than 0.05 was considered statistically significant. Because of the exploratory design, modest sample size, and age imbalance, adjusted and multiple-comparison-corrected results were prioritized over unadjusted p-values in interpretation.

RESULTS

Study Population and Clinical Characteristics

A total of 45 eyes were included in the analysis: 15 healthy control eyes, 15 eyes with pseudoexfoliation syndrome without glaucoma, and 15 eyes with pseudoexfoliation glaucoma. Demographic and clinical characteristics are summarized in Table 1.

The healthy group was substantially younger than both pseudoexfoliation groups, with mean age increasing from 23.3 ± 4.4 years in healthy controls to 58.1 ± 8.5 years in PEX and 65.5 ± 6.6 years in PEXG (Kruskal–Wallis $p < 0.001$). This age imbalance was considered a major interpretive factor and was addressed using age/sex-adjusted models. Sex-code distribution was identical across the three groups, with 8 eyes coded as sex category 1 and 7 eyes coded as sex category 2 in each group ($p = 1.000$).

Clinical severity markers showed the expected glaucoma-specific pattern. Best-corrected visual acuity differed across groups (0.12 ± 0.10, 0.58 ± 0.16, and 0.58 ± 0.17 logMAR in healthy, PEX, and PEXG eyes, respectively; $p < 0.001$; adjusted $p < 0.001$). Intraocular pressure was highest in PEXG eyes (13.1 ± 2.5, 14.1 ± 1.8, and 21.3 ± 4.9 mmHg; $p < 0.001$; adjusted $p < 0.001$). Cup-disc ratio also showed a marked glaucoma-specific increase, rising from 0.27 ± 0.09 in healthy eyes and 0.31 ± 0.10 in PEX eyes to 0.66 ± 0.16 in PEXG eyes ($p < 0.001$; adjusted $p < 0.001$).

Primary Domain-Level OCT/OCTA Findings

Domain-level OCT and OCTA findings are summarized in Table 2 and illustrated in Fig. 1. The clearest glaucoma-specific signal was observed for mean peripapillary RNFL thickness. Mean RNFL thickness decreased progressively across the PEX spectrum, from 90.3 ± 5.3 μm in healthy eyes to 82.0 ± 8.1 μm in PEX eyes and 61.8 ± 10.7 μm in PEXG eyes (Kruskal–Wallis $p < 0.001$; FDR $q < 0.001$; age/sex-adjusted $p < 0.001$; $\varepsilon^2 = 0.67$). Relative to healthy eyes, RNFL thickness was reduced by 9.2% in PEX and by 31.6% in PEXG. Holm-adjusted pairwise testing confirmed significant differences between healthy and PEX eyes ($p = 0.002$), healthy and PEXG eyes ($p < 0.001$), and PEX and PEXG eyes ($p < 0.001$).

Mean RPC vessel density was also lower in both PEX groups than in healthy eyes on unadjusted analysis. Mean RPC VD declined from 57.6 ± 7.1 in healthy eyes to 45.7 ± 8.9 in PEX and 43.9 ± 9.1 in PEXG ($p < 0.001$; FDR $q < 0.001$; $\varepsilon^2 = 0.34$), corresponding to reductions of 20.7% and 23.8% versus healthy eyes, respectively. However, the age/sex-adjusted group effect was not significant (adjusted p =

0.877), indicating that the RPC signal was strongly influenced by demographic imbalance. Pairwise testing showed lower RPC VD in PEX and PEXG compared with healthy eyes, but no significant difference between PEX and PEXG (p = 0.480).

Conjunctival OCTA domain indices showed a similar pattern to RPC VD. Mean conjunctival VD was reduced from 0.37 ± 0.03 in healthy eyes to 0.31 ± 0.05 in PEX and 0.29 ± 0.05 in PEXG (p < 0.001; FDR q < 0.001; ε^2 = 0.44), but the age/sex-adjusted group effect was not significant (adjusted p = 0.354). Mean conjunctival VLD was also lower across groups (0.20 ± 0.02, 0.16 ± 0.04, and 0.16 ± 0.04; p = 0.013; FDR q = 0.015; ε^2 = 0.16), but did not remain significant after adjustment (adjusted p = 0.474). Mean conjunctival VDI decreased from 1.96 ± 0.06 in healthy eyes to 1.74 ± 0.16 in PEX and 1.71 ± 0.14 in PEXG (p < 0.001; FDR q < 0.001; ε^2 = 0.47), with a borderline age/sex-adjusted group effect (adjusted p = 0.070).

Overall, Fig. 1 demonstrates two distinct patterns: RNFL thickness shows a progressive and glaucoma-specific decline from healthy to PEX to PEXG, whereas RPC and conjunctival OCTA indices are already reduced at the PEX stage and show limited additional decline in PEXG.

Peripapillary Sectoral Analysis

Peripapillary sectoral findings are presented in Table 3 and visualized in Fig. 2. All RNFL quadrants differed significantly across groups and remained significant after age/sex adjustment. In PEXG eyes, the largest RNFL reduction relative to healthy eyes was observed in the nasal quadrant (-35.9%), followed by the superior (-33.6%), inferior (-32.9%), and temporal (-21.2%) quadrants. In PEX eyes without glaucoma, RNFL reductions were smaller, ranging from − 4.3% temporally to -12.9% nasally.

In contrast, RPC vessel density showed significant unadjusted reductions in all sectors but did not retain significance after age/sex adjustment. Relative to healthy eyes, RPC VD reductions in PEX ranged from − 18.5% in the nasal sector to -22.7% in the temporal sector. In PEXG, reductions ranged from − 20.8% superiorly to -26.9% temporally. However, adjusted p-values for all RPC sectors were non-significant, ranging from 0.801 to 0.935.

Figure 2 highlights the divergence between structural and vascular peripapillary markers. RNFL sectors show a steep PEXG-specific gradient, whereas RPC VD reductions are already evident in PEX and show less disease-stage separation.

Conjunctival Sectoral OCTA Analysis

Conjunctival sectoral OCTA findings are summarized in Tables 4A–4C and illustrated in Fig. 3. Conjunctival vessel density was significantly lower in all four regions on unadjusted analysis. Compared with healthy eyes, PEXG eyes showed VD reductions of -19.9% in the nasal superficial region, -20.4% in the nasal deep region, -21.9% in the temporal superficial region, and − 21.6% in the temporal deep region. However, none of the conjunctival VD sectors remained significant after age/sex adjustment.

Conjunctival VLD showed significant unadjusted reductions in the nasal superficial, nasal deep, and temporal deep regions. The largest reduction was observed in temporal deep VLD, which decreased by 23.9% in PEX and 23.3% in PEXG compared with healthy eyes. Temporal superficial VLD did not remain significant after FDR correction. None of the VLD sectors remained significant after age/sex adjustment.

Conjunctival VDI showed the most consistent sectoral signal among conjunctival parameters. All four VDI sectors were reduced in PEX and PEXG compared with healthy eyes on unadjusted analysis. Importantly, two superficial VDI regions retained significance after age/sex adjustment: nasal superficial VDI (adjusted p = 0.030) and temporal superficial VDI (adjusted p = 0.018). Compared with healthy eyes, PEXG eyes showed VDI reductions of -13.7% nasally superficial, -11.7% nasally deep, -14.3% temporally superficial, and − 11.8% temporally deep.

Figure 3 demonstrates that conjunctival OCTA reductions were widespread across nasal and temporal, superficial and deep regions. However, the magnitude of reduction was similar in PEX and PEXG, indicating the limited ability of conjunctival OCTA to distinguish glaucoma conversion within the PEX spectrum.

Diagnostic Accuracy for PEX Glaucoma

ROC analysis for distinguishing PEXG from non-glaucomatous eyes is shown in Table 5 and Fig. 4. Mean RNFL thickness had the strongest diagnostic performance, with an AUC of 0.96 (bootstrap 95% CI, 0.90–1.00). The optimal Youden cutoff was 77.2 μm, yielding a sensitivity of 0.93 and a specificity of 0.90.

Traditional clinical markers also performed strongly. Cup-disc ratio had an AUC of 0.94 (95% CI, 0.81–1.00), with an optimal cutoff of 0.50, sensitivity of 0.93, and specificity of 0.93. IOP had an AUC of 0.93 (95% CI, 0.83–0.99), with an optimal cutoff of 18.0 mmHg, sensitivity of 0.73, and specificity of 1.00.

OCTA vascular indices showed lower diagnostic performance than RNFL thickness. Mean conjunctival VDI had moderate discrimination for PEXG, with an AUC of 0.77 (95% CI, 0.61–0.90), followed by mean conjunctival VD with an AUC of 0.76 (95% CI, 0.60–0.89), mean RPC VD with an AUC of 0.73 (95% CI, 0.56–0.88), and mean conjunctival VLD with an AUC of 0.61 (95% CI, 0.43–0.79).

As shown in Fig. 4, the RNFL curve was clearly separated from the vascular OCTA curves, supporting RNFL thickness as the dominant diagnostic marker for PEXG in this dataset.

Correlations Between Clinical Severity Markers and OCT/OCTA Domains

Spearman correlation analyses are summarized in Table 6 and Fig. 5. Mean RNFL thickness showed significant inverse correlations with all major clinical severity markers: BCVA (rho = -0.54), IOP (rho = -0.58), cup-disc ratio (rho = -0.61), and age (rho = -0.66), all $p < 0.05$. These findings indicate that a thinner RNFL was associated with worse visual acuity, higher IOP, larger cup-disc ratio, and older age.

Mean RPC VD was significantly correlated with BCVA (rho = -0.53), IOP (rho = -0.32), and age (rho = -0.60). Mean conjunctival VD correlated with BCVA (rho = -0.37), cup-disc ratio (rho = -0.49), and age (rho = -0.58). Mean conjunctival VDI correlated with BCVA (rho = -0.33), IOP (rho = -0.31), cup-disc ratio (rho = -0.42), and age (rho = -0.59). Mean conjunctival VLD showed a weaker association profile and correlated significantly only with age (rho = -0.34).

Figure 5 emphasizes that age was consistently associated with lower OCTA vascular values across both peripapillary and conjunctival domains. This reinforces the need to interpret vascular OCTA findings cautiously in the presence of age imbalance.

Impact of Age/Sex Adjustment

The impact of age/sex adjustment is summarized in Fig. 6. Structural RNFL parameters remained robust after adjustment, with mean RNFL and all RNFL quadrants retaining statistical significance. In contrast, mean RPC VD and all RPC sectoral parameters lost significance after adjustment. Similarly, mean conjunctival VD, VLD, and VDI did not remain independently significant at the domain level, although nasal superficial and temporal superficial VDI retained exploratory significance at the sectoral level.

These adjusted analyses indicate that the most reliable disease-specific finding was peripapillary RNFL thinning, whereas vascular-domain findings were substantially influenced by age. Therefore, RPC and conjunctival OCTA abnormalities should be interpreted as exploratory microvascular signals requiring validation in age-matched cohorts.

Table 1
Demographic and Clinical Characteristics

Variable	Healthy (n = 15)	PEX (n = 15)	PEX Glaucoma (n = 15)	KW p	Age/Sex-Adjusted p
Age, years	23.3 ± 4.4	58.1 ± 8.5	65.5 ± 6.6	< 0.001	—
Sex code (1:2)	8:7	8:7	8:7	1.000	—
BCVA, logMAR	0.12 ± 0.10	0.58 ± 0.16	0.58 ± 0.17	< 0.001	< 0.001
IOP, mmHg	13.1 ± 2.5	14.1 ± 1.8	21.3 ± 4.9	< 0.001	< 0.001
Cup-disc ratio	0.27 ± 0.09	0.31 ± 0.10	0.66 ± 0.16	< 0.001	< 0.001

Values mean ± SD. Sex codes 1 and 2 used as provided; adjusted statistically without biological interpretation. KW = Kruskal-Wallis; BCVA = best-corrected visual acuity; IOP = intraocular pressure.

Table 2
Primary Peripapillary and Conjunctival OCT/OCTA Domain-Level Findings

Domain Index	Healthy	PEX	PEX Glaucoma	KW p	FDR q	Adjusted p	ε^2	%Δ vs. Healthy
Mean RNFL, µm	90.3 ± 5.3	82.0 ± 8.1	61.8 ± 10.7	< 0.001	< 0.001	< 0.001	0.67	PEX − 9.2%; PEXG − 31.6%
Mean RPC VD	57.6 ± 7.1	45.7 ± 8.9	43.9 ± 9.1	< 0.001	< 0.001	0.877	0.34	PEX − 20.7%; PEXG − 23.8%
Mean Conj VD	0.37 ± 0.03	0.31 ± 0.05	0.29 ± 0.05	< 0.001	< 0.001	0.354	0.44	PEX − 17.2%; PEXG − 20.9%
Mean Conj VLD	0.20 ± 0.02	0.16 ± 0.04	0.16 ± 0.04	0.013	0.015	0.474	0.16	PEX − 18.6%; PEXG − 17.0%
Mean Conj VDI	1.96 ± 0.06	1.74 ± 0.16	1.71 ± 0.14	< 0.001	< 0.001	0.070	0.47	PEX − 11.3%; PEXG − 12.9%

RNFL: Retinal Nerve Fiber Layer, RPC VD: radial peripapillary capillaries vessel density, VLD: vascular length density, VDI; Vascular density Index

Table 3
Peripapillary Sectoral Variables

Variable	Healthy	PEX	PEX Glaucoma	KW p	FDR q	Adjusted p	PEX %Δ	PEXG %Δ
RNFL								
Superior	103.1 ± 5.6	93.1 ± 9.3	68.4 ± 11.2	< 0.001	< 0.001	< 0.001	-9.6%	-33.6%
Inferior	106.9 ± 5.2	97.2 ± 8.3	71.7 ± 11.5	< 0.001	< 0.001	< 0.001	-9.0%	-32.9%
Temporal	67.5 ± 6.7	64.6 ± 7.2	53.2 ± 10.2	< 0.001	< 0.001	< 0.001	-4.3%	-21.2%
Nasal	83.9 ± 5.8	73.1 ± 9.8	53.8 ± 11.9	< 0.001	< 0.001	< 0.001	-12.9%	-35.9%
RPC VD								
Superior	57.6 ± 8.1	46.4 ± 7.8	45.6 ± 7.6	< 0.001	< 0.001	0.830	-19.4%	-20.8%
Inferior	60.7 ± 7.5	47.3 ± 10.4	45.4 ± 10.9	< 0.001	< 0.001	0.891	-22.1%	-25.2%
Nasal	55.5 ± 7.1	45.3 ± 8.4	43.2 ± 8.7	0.001	0.001	0.935	-18.5%	-22.2%
Temporal	56.5 ± 6.4	43.7 ± 9.3	41.3 ± 9.8	< 0.001	< 0.001	0.801	-22.7%	-26.9%

RNFL: Retinal Nerve Fiber Layer, RPC VD: radial peripapillary capillaries vessel density, KW: Kruskal-Wallis, FDR: false discovery rate

Table 4
A. Conjunctival Vessel Density Sectoral Findings

Variable	Healthy	PEX	PEX Glaucoma	KW p	FDR q	Adjusted p	PEX %Δ	PEXG %Δ
VD Nasal S/S	0.381 ± 0.037	0.319 ± 0.066	0.305 ± 0.069	0.002	0.003	0.510	-16.3%	-19.9%
VD Nasal Deep	0.379 ± 0.046	0.315 ± 0.050	0.301 ± 0.058	< 0.001	< 0.001	0.407	-16.7%	-20.4%
VD Temporal S/S	0.380 ± 0.042	0.304 ± 0.049	0.297 ± 0.053	< 0.001	< 0.001	0.333	-20.0%	-21.9%
VD Temporal Deep	0.353 ± 0.043	0.297 ± 0.070	0.277 ± 0.063	< 0.001	< 0.001	0.648	-15.9%	-21.6%

Table 4
B. Conjunctival Vessel Length Density Sectoral Findings

Variable	Healthy	PEX	PEX Glaucoma	KW p	FDR q	Adjusted p	PEX %Δ	PEXG %Δ
VLD Nasal S/S	0.199 ± 0.017	0.163 ± 0.038	0.167 ± 0.038	0.006	0.008	0.218	-17.8%	-15.8%
VLD Nasal Deep	0.190 ± 0.023	0.158 ± 0.039	0.162 ± 0.039	0.029	0.031	0.593	-16.8%	-14.7%
VLD Temporal S/S	0.192 ± 0.021	0.162 ± 0.051	0.165 ± 0.057	0.073	0.073	0.835	-15.6%	-13.9%
VLD Temporal Deep	0.203 ± 0.029	0.155 ± 0.043	0.156 ± 0.042	0.002	0.003	0.352	-23.9%	-23.3%

Table 4
C. Conjunctival Vessel Density Index Sectoral Findings

Variable	Healthy	PEX	PEX Glaucoma	KW p	FDR q	Adjusted p	PEX %Δ	PEXG %Δ
VDI Nasal S/S	2.00 ± 0.09	1.77 ± 0.18	1.72 ± 0.12	< 0.001	< 0.001	0.030	-11.3%	-13.7%
VDI Nasal Deep	1.95 ± 0.08	1.73 ± 0.18	1.72 ± 0.16	< 0.001	< 0.001	0.138	-11.3%	-11.7%
VDI Temporal S/S	1.97 ± 0.06	1.72 ± 0.16	1.69 ± 0.14	< 0.001	< 0.001	0.018	-12.8%	-14.3%
VDI Temporal Deep	1.94 ± 0.08	1.75 ± 0.19	1.71 ± 0.19	0.001	0.002	0.638	-9.8%	-11.8%

RNFL: Retinal Nerve Fiber Layer, RPC VD: radial peripapillary capillaries vessel density, KW: Kruskal-Wallis, FDR: false discovery rate, VLD: vascular length density, VDI; Vascular density Index

Table 5
ROC Analysis for PEX Glaucoma vs. Non-Glaucoma

Predictor	AUC	Bootstrap 95% CI	Youden Cutoff	Sensitivity	Specificity
Mean RNFL Thickness	0.96	0.90-1.00	77.2 µm	0.93	0.90
Cup-Disc Ratio	0.94	0.81-1.00	0.50	0.93	0.93
IOP	0.93	0.83–0.99	18.0 mmHg	0.73	1.00
Mean Conj VDI	0.77	0.61–0.90	1.808	0.87	0.63
Mean Conj VD	0.76	0.60–0.89	0.365	1.00	0.43
Mean RPC VD	0.73	0.56–0.88	51.5	0.87	0.57
Mean Conj VLD	0.61	0.43–0.79	0.158	0.47	0.77

RNFL: Retinal Nerve Fiber Layer, RPC: radial peripapillary capillaries VD: vessel density, VLD: vascular length density, VDI; Vascular density Index,

Table 6
Spearman Correlations Between Clinical Variables and Domain-Level Indices

Clinical Variable	Mean RNFL	Mean RPC VD	Conj VD	Conj VLD	Conj VDI
BCVA	-0.54*	-0.53*	-0.37*	-0.29	-0.33*
IOP	-0.58*	-0.32*	-0.25	0.02	-0.31*
Cup-Disc Ratio	-0.61*	-0.27	-0.49*	-0.18	-0.42*
Age	-0.66*	-0.60*	-0.58*	-0.34*	-0.59*

RNFL: Retinal Nerve Fiber Layer, RPC: radial peripapillary capillaries VD: vessel density, VLD: vascular length density, VDI; Vascular density Index, IOP; intraocular pressure

*Values are Spearman rho. *$p < 0.05$. Negative correlations reflect lower OCT/OCTA values with worse clinical parameters or older age.*

DISCUSSION

In this two-domain OCT/OCTA analysis of the pseudoexfoliation spectrum, three principal findings emerged. First, peripapillary RNFL thickness was the most robust and glaucoma-specific biomarker, showing progressive reduction from healthy eyes to PEX eyes and then to PEXG eyes. This effect persisted after age/sex adjustment and demonstrated excellent diagnostic accuracy for PEXG. Second, the mean RPC vessel density was lower in both PEX and PEXG eyes compared with healthy eyes in unadjusted analyses, but this effect was not significant after age/sex adjustment, indicating that the vascular signal is strongly influenced by age in the present dataset. Third, conjunctival OCTA indices

were reduced in both PEX and PEXG eyes compared with healthy eyes, with limited separation between PEX and PEXG. Together, these findings suggest that RNFL thinning is the dominant marker of glaucomatous conversion, whereas RPC and conjunctival OCTA abnormalities may reflect broader pseudoexfoliation-related microvascular involvement that requires age-matched validation.

The strongest result of the study was the progressive RNFL reduction across disease groups. Mean RNFL thickness decreased from 90.3 μm in healthy eyes to 82.0 μm in PEX eyes and 61.8 μm in PEXG eyes, with a large effect size and persistence after age/sex adjustment. ROC analysis further supported the clinical strength of RNFL, with an AUC of 0.96 for distinguishing PEXG from non-glaucomatous eyes. This diagnostic performance exceeded that of mean RPC vessel density and conjunctival OCTA indices and was comparable to traditional clinical severity markers such as cup-disc ratio and IOP. These findings are consistent with the established role of RNFL thickness as a primary structural marker of glaucomatous optic neuropathy and support its continued central role in PEXG evaluation.

The sectoral RNFL results further reinforce this interpretation. The largest reductions in PEXG were observed in the nasal, superior, and inferior quadrants, while the temporal quadrant showed a smaller but still significant reduction. This pattern is compatible with glaucomatous axonal loss, in which superior and inferior arcuate fiber bundles are commonly affected. Figure 2 illustrates this clearly: RNFL sectors show a steep PEX-to-PEXG gradient, whereas RPC reductions are already present in PEX and show less additional decline in PEXG. This distinction is important because it suggests that RNFL provides the clearest glaucoma-specific separation in this dataset, while peripapillary vascular loss may be less specific or more strongly confounded by age.

The RPC findings should therefore be interpreted cautiously. Mean RPC vessel density was substantially lower in PEX and PEXG eyes compared with healthy eyes in unadjusted analyses, with reductions of approximately 20.7% and 23.8%, respectively. However, the age/sex-adjusted group effect was not significant. This attenuation does not exclude a disease-related vascular component in PEX; rather, it indicates that the present dataset cannot confidently separate disease effects from age-related vascular changes. This is particularly important because the healthy group was much younger than both PEX groups, and age correlated negatively with mean RPC vessel density. In other words, the unadjusted RPC difference may represent a mixture of pseudoexfoliation-related microvascular compromise and physiological age-related reduction in OCTA-derived vessel density.

Prior OCTA studies provide useful context for this finding. Ahoor et al. reported lower peripapillary vessel density in PEXG compared with PEX and controls and found a strong relationship between peripapillary vessel density and RNFL thickness [17]. Khalouli et al. similarly showed that circumpapillary vessel density was reduced in manifest glaucoma and correlated with structural parameters, but their findings also suggested that vascular loss may be more evident after structural damage is established [18]. In contrast, Aribas et al. reported reduced peripapillary vessel density in PEX eyes despite similar RNFL thickness compared with controls, supporting the possibility that vascular changes may occur before detectable structural thinning in some PEX eyes [19]. The present study does not resolve this temporal

question because of its cross-sectional design and age imbalance. However, it supports the concept that peripapillary vascular measures are biologically relevant in PEX and should be evaluated in larger age-matched longitudinal cohorts.

The most novel component of this study is the conjunctival OCTA analysis. Mean conjunctival VD, VLD, and VDI were lower in both PEX and PEXG eyes compared with healthy eyes, and Fig. 3 demonstrates that these reductions were present across nasal and temporal, superficial and deep regions. However, conjunctival OCTA parameters showed limited PEX-to-PEXG separation. This pattern suggests that conjunctival microvascular alteration may be a marker of PEX-related ocular-surface or anterior-segment disease burden rather than a marker of glaucomatous conversion itself. This interpretation is biologically plausible because pseudoexfoliative material has been identified in conjunctival and extrabulbar tissues, and PEX is increasingly understood as a systemic elastotic microfibrillopathy rather than an isolated anterior-chamber disorder [1, 3, 6, 7].

Among conjunctival parameters, VDI may be the most promising exploratory metric. Although mean conjunctival VDI did not reach conventional significance after age/sex adjustment, it approached significance and showed moderate diagnostic discrimination. Sectorally, nasal superficial and temporal superficial VDI remained significant after adjustment, although these findings should be interpreted as exploratory because of the small sample size and multiple regional comparisons. VDI may be less vulnerable than simple vessel density to certain image-processing or vessel-caliber effects because it reflects a composite vascular index rather than vessel area alone. However, this interpretation remains speculative until conjunctival OCTA acquisition, segmentation, thresholding, and repeatability are standardized in PEX populations.

The diagnostic analysis provides a clinically useful hierarchy of biomarkers. Figure 4 shows that mean RNFL thickness had excellent discrimination for PEXG, with an AUC of 0.96, followed by cup-disc ratio and IOP. In contrast, conjunctival VDI and VD showed only moderate discrimination, while mean RPC vessel density showed moderate-to-lower performance. These results indicate that conjunctival OCTA should not be presented as a replacement for RNFL, IOP, optic disc evaluation, or visual field testing in PEXG diagnosis. Its potential value is different: it may provide an exploratory anterior-segment microvascular signal of PEX involvement, possibly useful for disease phenotyping or for studying systemic vascular associations of PEX.

The correlation findings also support this cautious interpretation. Mean RNFL correlated with BCVA, IOP, cup-disc ratio, and age, consistent with its relationship to clinical disease severity. Mean RPC vessel density and conjunctival vascular indices also correlated with age, and conjunctival VD correlated with cup-disc ratio. Figure 5 highlights the central challenge of interpretation: vascular OCTA measures are related both to disease markers and to age. Therefore, vascular findings in the present study should be considered hypothesis-generating rather than definitive evidence of independent PEX-related microvascular pathology. The most defensible conclusion is that vascular OCTA changes are detectable

in the PEX spectrum, but their independence from age and their specificity for glaucoma require validation.

Based on these findings and the prior literature, a two-domain model can be proposed. The posterior peripapillary domain, especially RNFL thickness, primarily reflects glaucomatous neuroaxonal damage and is most useful for identifying PEXG. RPC vessel density may reflect the vascular component of optic nerve head vulnerability, but in this study, it was not independently glaucoma-specific after age/sex adjustment. The anterior conjunctival domain may reflect pseudoexfoliation-related ocular-surface or extrabulbar microvascular involvement. Under this model, conjunctival OCTA is not a direct glaucoma diagnostic test; rather, it may represent a novel window into the systemic/anterior-segment vascular component of PEX. This model is consistent with the systemic nature of PEX and with histopathological evidence of conjunctival and extrabulbar pseudoexfoliative deposition.

This study has several strengths. It separates posterior peripapillary biomarkers from anterior conjunctival OCTA biomarkers, which allows clearer interpretation of structural glaucoma damage versus broader microvascular involvement. It includes domain-level and sectoral analyses, correction for multiple testing, age/sex-adjusted models, correlation analysis, and ROC analysis. The figures provide a coherent visual summary: Fig. 1 shows the domain-level pattern, Fig. 2 emphasizes the glaucoma-specific RNFL gradient, Fig. 3 demonstrates widespread conjunctival vascular reduction in both PEX groups, Fig. 4 establishes RNFL as the strongest diagnostic classifier, and Fig. 5 shows the importance of age as a vascular confounder. The inclusion of conjunctival OCTA is particularly novel and provides a foundation for future anterior-segment vascular studies in PEX.

Several limitations must be emphasized. The most important limitation is the substantial age imbalance between healthy controls and the PEX groups. Because both PEX prevalence and OCTA-derived vascular parameters are age-sensitive, this imbalance limits causal and disease-specific interpretation of RPC and conjunctival vascular findings. Although age- and sex-adjusted models were used, statistical adjustment cannot fully replace an age-matched study design, especially with only 15 eyes per group. Second, the cross-sectional design prevents determination of whether vascular changes precede RNFL thinning, occur secondary to glaucomatous damage, or reflect generalized age-related microvascular change. Third, the sample size limits multivariable modeling and makes ROC thresholds preliminary. Fourth, important potential confounders—including axial length, ocular perfusion pressure, systemic vascular risk factors, topical glaucoma medication exposure, OCTA signal strength, and detailed image-quality grading—were not fully available. Fifth, conjunctival OCTA remains technically and methodologically less standardized than posterior-segment OCTA, and reproducibility data specific to PEX are lacking. Finally, no macular OCTA or visual field indices were available for integrated structure–function–vascular modeling; therefore, macular conclusions should not be drawn from this dataset.

Conclusion

In conclusion, this two-domain OCT/OCTA analysis indicates that peripapillary RNFL thickness is the dominant glaucoma-specific biomarker in the PEX spectrum, with excellent diagnostic accuracy for PEXG. RPC vessel density and conjunctival OCTA indices were reduced in PEX and PEXG eyes in unadjusted analyses, suggesting possible microvascular involvement by the PEX stage. Still, these vascular findings were strongly influenced by age and did not provide a clear independent separation of PEXG from PEX. Conjunctival OCTA should therefore be framed as a novel exploratory anterior-segment microvascular marker of pseudoexfoliation-related disease burden rather than a validated diagnostic biomarker for glaucoma. Larger age-matched, longitudinal, multimodal studies are required to determine whether conjunctival OCTA can predict PEX progression, reflect systemic vascular involvement, or complement established structural and functional markers in clinical risk stratification.

Declarations

Author contributions

AM conceptualized and designed the work. AM, MH, NM, and FN assessed the patients and analysed the data. AM drafted the main manuscript text, and MH critically revised the manuscript. We extend our appreciation to Professor Majid Navaei of Amirkabir University for providing statistical consultation and analysis.

Consent for publication

Not Applicable

Funding

Non

Data availability statement

Data will be available on request from the corresponding author.

Conflict of interest

The authors declare that they have no known competing financial interests or personal relationships that could have appeared to influence the work reported in this paper.

Consent to participate statement

Written informed consent was obtained from all participants.

References

1. -Ahoor MH, Sorkhabi R, Najafzadeh F, Mahmoudzadeh S, Arasteh A, Gharamaleki A, T. Comparison of retinal and choroidal vascular changes via optical coherence tomography angiography between pseudoexfoliative glaucoma and pseudoexfoliation syndrome and control group. Photodiagn Photodyn Ther. 2025;51:104444. https://doi.org/10.1016/j.pdpdt.2024.104444.
2. -Akagi T, Uji A, Huang AS, Weinreb RN, Yamada T, Miyata M, Kameda T, Ikeda HO, Tsujikawa A. Conjunctival and intrascleral vasculatures assessed using anterior-segment optical coherence tomography angiography in normal eyes. Am J Ophthalmol. 2018;196:1–9. https://doi.org/10.1016/j.ajo.2018.08.009.
3. -Anderson DR, Hendrickson A. Effect of intraocular pressure on rapid axoplasmic transport in monkey optic nerve. Invest Ophthalmol. 1974;13(10):771–83.
4. -Aribas YK, Aktas Z, Segewa A. Evaluating peripapillary vessel density and retinal nerve fiber layer thickness in pseudoexfoliation syndrome: A comparative study. Turkish J Clin Experimental Ophthalmol. 2025;20(2):93–9. https://doi.org/10.37844/TJ-CEO.2025.20.15.
5. -Cai S, Zhao F, Du C. Repeatability of ocular surface vessel density measurements with optical coherence tomography angiography. BMC Ophthalmol. 2019;19:248. https://doi.org/10.1186/s12886-019-1255-2.
6. -Chae SB, Kim JL. Optical coherence tomography angiography analysis of the fellow eye in unilateral pseudoexfoliation syndrome. BMC Ophthalmol. 2024;24:421. https://doi.org/10.1186/s12886-024-03686-1.
7. -Chatziralli I, Milionis I, Christodoulou A, Theodossiadis P, Kitsos G. The role of vessel density as measured by optical coherence tomography angiography in the evaluation of pseudoexfoliative glaucoma: A review of the literature. Ophthalmol Therapy. 2022;11(2):533–45. https://doi.org/10.1007/s40123-022-00483-1.
8. -Dikmetas O, Sadigh SL, Şekerler C, Kocabeyoğlu S, Karahan S, Cankaya AB. Optic nerve head microvascular characteristics in patients with unilateral pseudoexfoliation syndrome: An optical coherence tomography angiography study. Int Ophthalmol. 2022;42(8):2397–405. https://doi.org/10.1007/s10792-022-02239-z.
9. -Elhawy E, Kamthan G, Dong CQ, Danias J. Pseudoexfoliation syndrome, a systemic disorder with ocular manifestations. Hum Genomics. 2012;6:22. https://doi.org/10.1186/1479-7364-6-22.
10. -Gillies WE, Brooks AMV. Central retinal vein occlusion in pseudoexfoliation of the lens capsule. Clin Exp Ophthalmol. 2002;30(3):176–87. https://doi.org/10.1046/j.1442-9071.2002.00513.x.
11. -Guemes-Villahoz N, Burgos-Blasco B, Fernández-Vigo JI, Morales-Fernández L, Perez-García P, García-Feijóo J, Martínez-de-la-Casa JM. Diagnostic ability of vessel density of the optic nerve head and macula versus structural parameters with optical coherence tomography in pseudoexfoliative glaucoma. Arch de la Sociedad Española de Oftalmología (English Edition). 2023;98(12):680–6. https://doi.org/10.1016/j.oftale.2023.09.004.
12. -Henkind P. Radial peripapillary capillaries of the retina. I. Anatomy: Human and comparative. *British J Ophthalmol 51*. 1967;2115–23. https://doi.org/10.1136/bjo.51.2.115.

13. -Jia Y, Wei E, Wang X, Zhang X, Morrison JC, Parikh M, Lombardi LH, Gattey DM, Armour RL, Edmunds B, Kraus MF, Fujimoto JG, Huang D. Optical coherence tomography angiography of optic disc perfusion in glaucoma. Ophthalmology. 2014;121(7):1322–32. https://doi.org/10.1016/j.ophtha.2014.01.021.
14. -Khallouli A, Oueslati Y, Gouider D, Bouchoucha S, Maalej A, Rannen R. Diagnostic accuracy and relationship between optical coherence tomography angiography vessel density and structural/functional parameters in healthy, preperimetric, and manifest glaucoma eyes. J Curr Ophthalmol. 2022;34(2):173–9. https://doi.org/10.4103/joco.joco_326_21.
15. -Lee BJH, Tey KY, Cheong EZK, Wong QY, Chua CSQ, Ang M. Anterior segment optical coherence tomography angiography: A review of applications for the cornea and ocular surface. Medicina. 2024;60(10):1597. https://doi.org/10.3390/medicina60101597.
16. -Liu L, Jia Y, Takusagawa HL, Pechauer AD, Edmunds B, Lombardi L, Davis E, Morrison JC, Huang D, Ophthalmology. 133(9), 1045–52. https://doi.org/10.1001/jamaophthalmol.2015.2225
17. -Liu Z, Wang H, Jiang H, Gameiro GR, Wang J. Quantitative analysis of conjunctival microvasculature imaged using optical coherence tomography angiography. Eye Vis. 2019;6:5. https://doi.org/10.1186/s40662-019-0130-9.
18. -Mohammadi A, Masihpour N, Hajizadeh M, Salehzadeh Z. Investigation of conjunctival vasculature changes assessed by anterior segment optical coherence tomography angiography after photorefractive keratectomy: A pilot study. Int Ophthalmol. 2026;46:29. https://doi.org/10.1007/s10792-025-03905-8.
19. -Park J-H, Yoo C, Girard MJA, Mari J-M, Kim YY. Peripapillary vessel density in glaucomatous eyes: Comparison between pseudoexfoliation glaucoma and primary open-angle glaucoma. J Glaucoma. 2018;27(11):1009–16. https://doi.org/10.1097/IJG.0000000000001062.
20. -Ritch R, Schlötzer-Schrehardt U. Exfoliation syndrome. Surv Ophthalmol. 2001;45(4):265–315. https://doi.org/10.1016/S0039-6257(00)00196-X.
21. -Schlötzer-Schrehardt U, Küchle M, Naumann GOH. Electron-microscopic identification of pseudoexfoliation material in extrabulbar tissue. Arch Ophthalmol. 1991;109(4):565–70. https://doi.org/10.1001/archopht.1991.01080040133044.
22. -Schlötzer-Schrehardt U, Naumann GOH. Ocular and systemic pseudoexfoliation syndrome. Am J Ophthalmol. 2006;141(5):921–37. https://doi.org/10.1016/j.ajo.2006.01.047.
23. -Sener H, Polat OA, Güray Sener AB. Optic nerve head vessel density in patients with pseudoexfoliation syndrome/glaucoma: A systematic review and meta-analysis. Photodiagn Photodyn Ther. 2023;42:103514. https://doi.org/10.1016/j.pdpdt.2023.103514.
24. -Simsek M, Inam O, Sen E, Elgin U. Analysis of the choroidal vascularity in asymmetric pseudoexfoliative glaucoma using optical coherence tomography-based image binarization. Eye. 2022;36(8):1615–22. https://doi.org/10.1038/s41433-021-01700-0.
25. -Streeten BW, Bookman L, Ritch R, Prince AM, Dark AJ. Pseudoexfoliative fibrillopathy in the conjunctiva: A relation to elastic fibers and elastosis. Ophthalmology. 1987;94(11):1439–49.

https://doi.org/10.1016/S0161-6420(87)33268-3.

26. -Tangtammaruk P, Petpiroon P, Supakonatanasan W, Teekhasaenee C, Suwan Y. Peripapillary perfused capillary density in true versus pseudoexfoliation syndrome: An OCTA study. PLoS ONE. 2020;15(12):e0239109. https://doi.org/10.1371/journal.pone.0239109.
27. -Tomczyk-Socha M, Tomczak W, Winkler-Lach W, Turno-Kręcicka A. Pseudoexfoliation syndrome—Clinical characteristics of most common cause of secondary glaucoma. J Clin Med. 2023;12(10):3580. https://doi.org/10.3390/jcm12103580.
28. -Werner AC, Shen LQ. A review of OCT angiography in glaucoma. Semin Ophthalmol. 2019;34(4):279–86. https://doi.org/10.1080/08820538.2019.1620807.
29. -Yüksel N, Karabaş VL, Arslan A, Demirci A, Çağlar Y. Ocular hemodynamics in pseudoexfoliation syndrome and pseudoexfoliation glaucoma. Ophthalmology. 2001;108(6):1043–9. https://doi.org/10.1016/S0161-6420(01)00572-3.
30. -Yüksel N, Yılmaz Tuğan B. Pseudoexfoliation glaucoma: Clinical presentation and therapeutic options. Turkish J Ophthalmol. 2023;53(4):247–56. https://doi.org/10.4274/tjo.galenos.2023.76300.

Figures

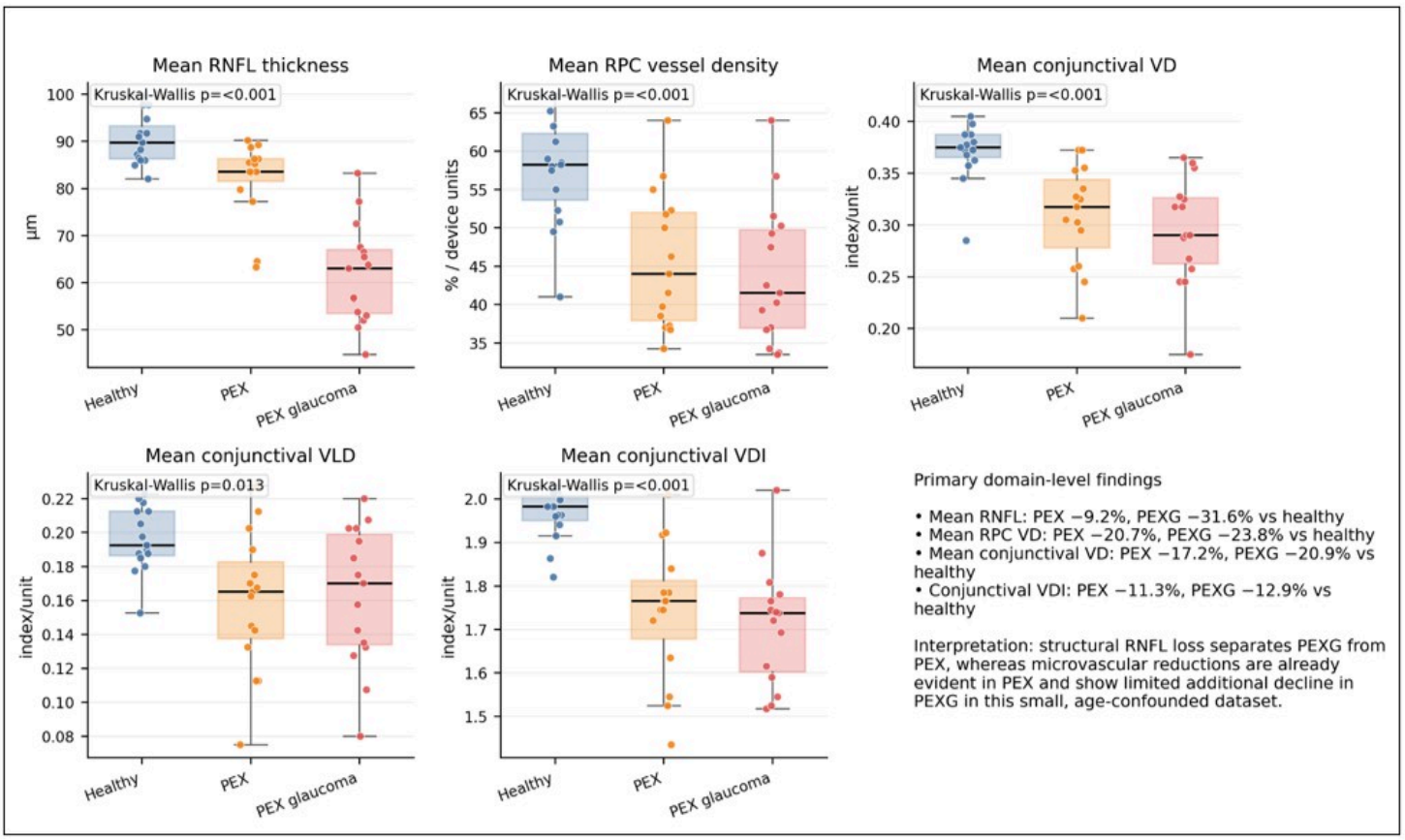


Figure 1

Domain-level OCT/RPC and conjunctival OCTA profile across groups. RNFL shows the steepest PEXG gradient; RPC and conjunctival indices are lower by the PEX stage.

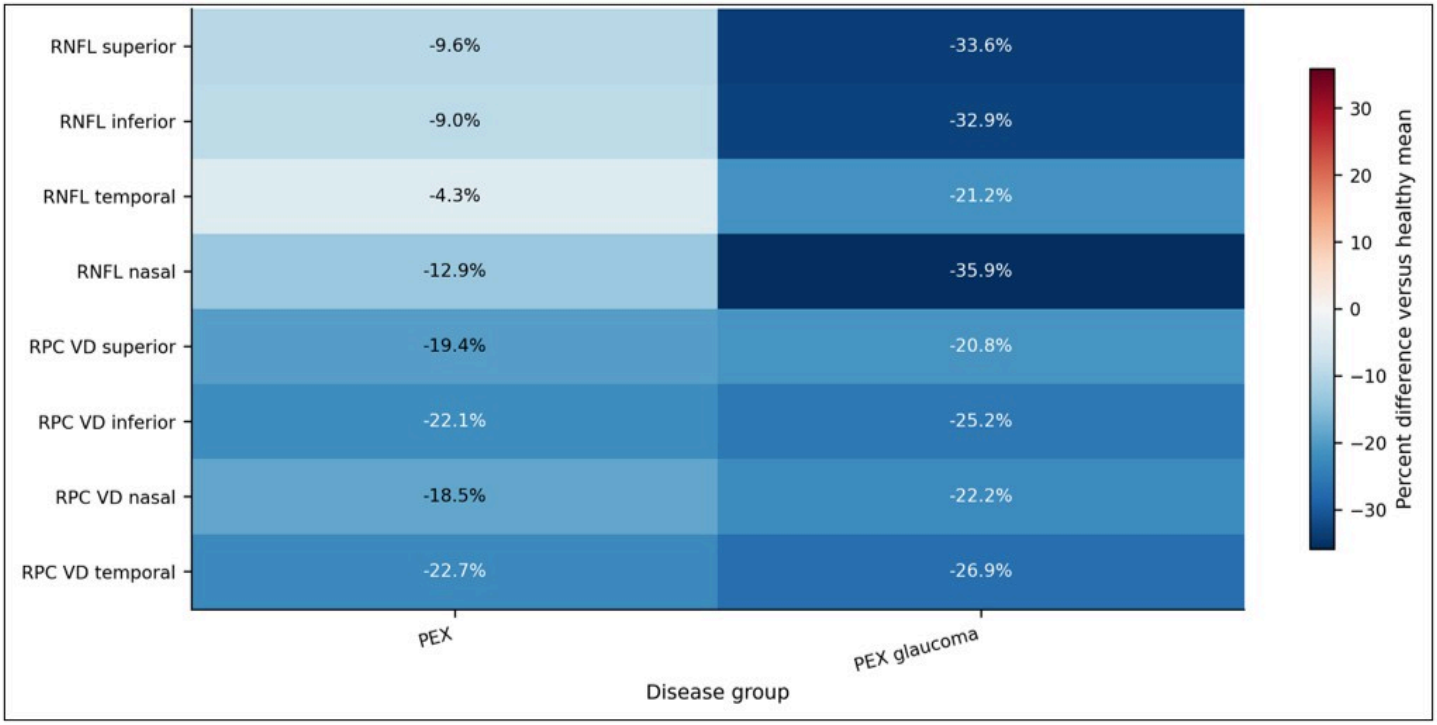


Figure 2

Peripapillary sectoral percentage change versus healthy eyes. RNFL shows the clearest glaucoma-specific gradient; RPC reduction is already present in PEX.

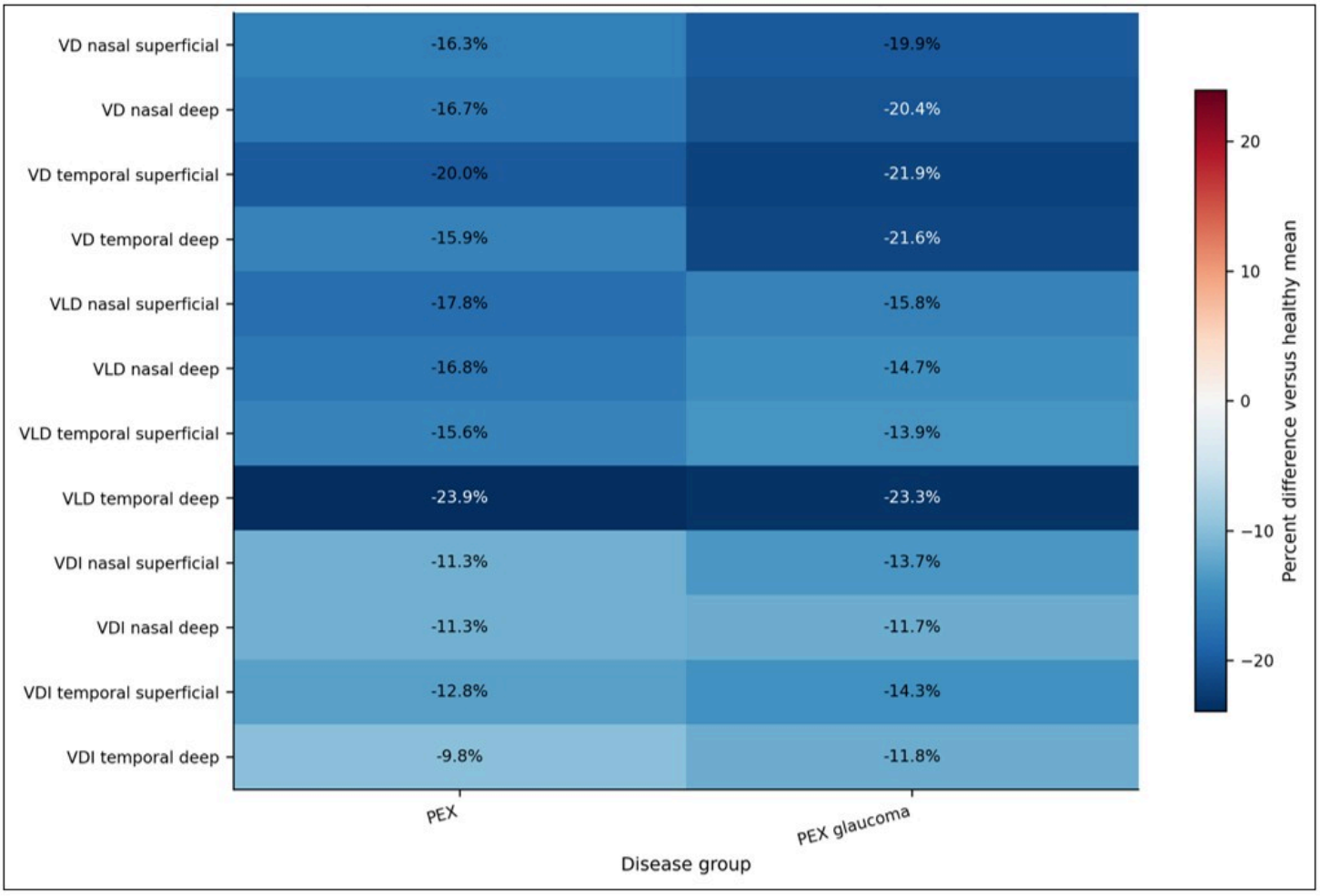


Figure 3

Conjunctival OCTA sectoral percentage change versus healthy eyes. Conjunctival VD, VLD, and VDI are lower in both PEX groups, with limited PEX-to-PEXG separation.

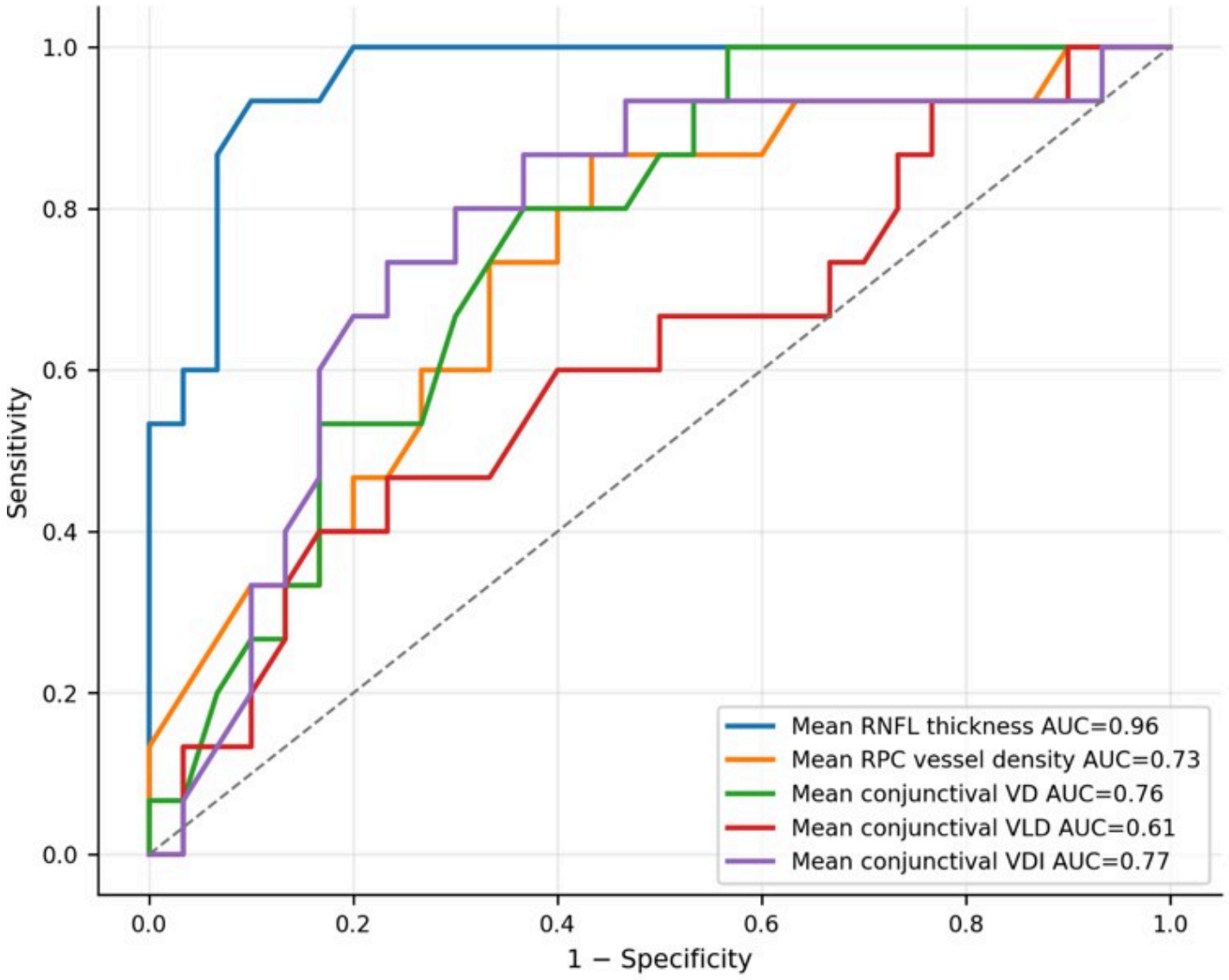


Figure 4

ROC curves for PEX glaucoma versus non-glaucoma. Mean RNFL thickness shows the strongest diagnostic accuracy.

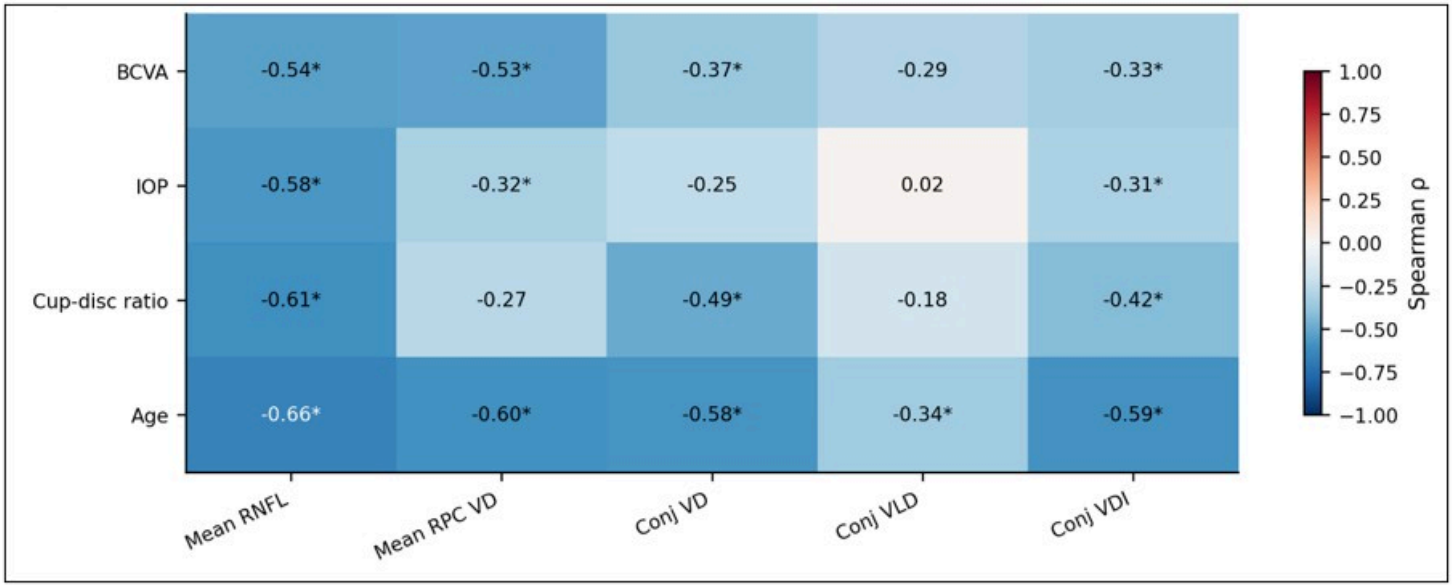


Figure 5

Spearman correlation heatmap. RNFL relates strongly to severity markers; vascular measures also correlate with age.

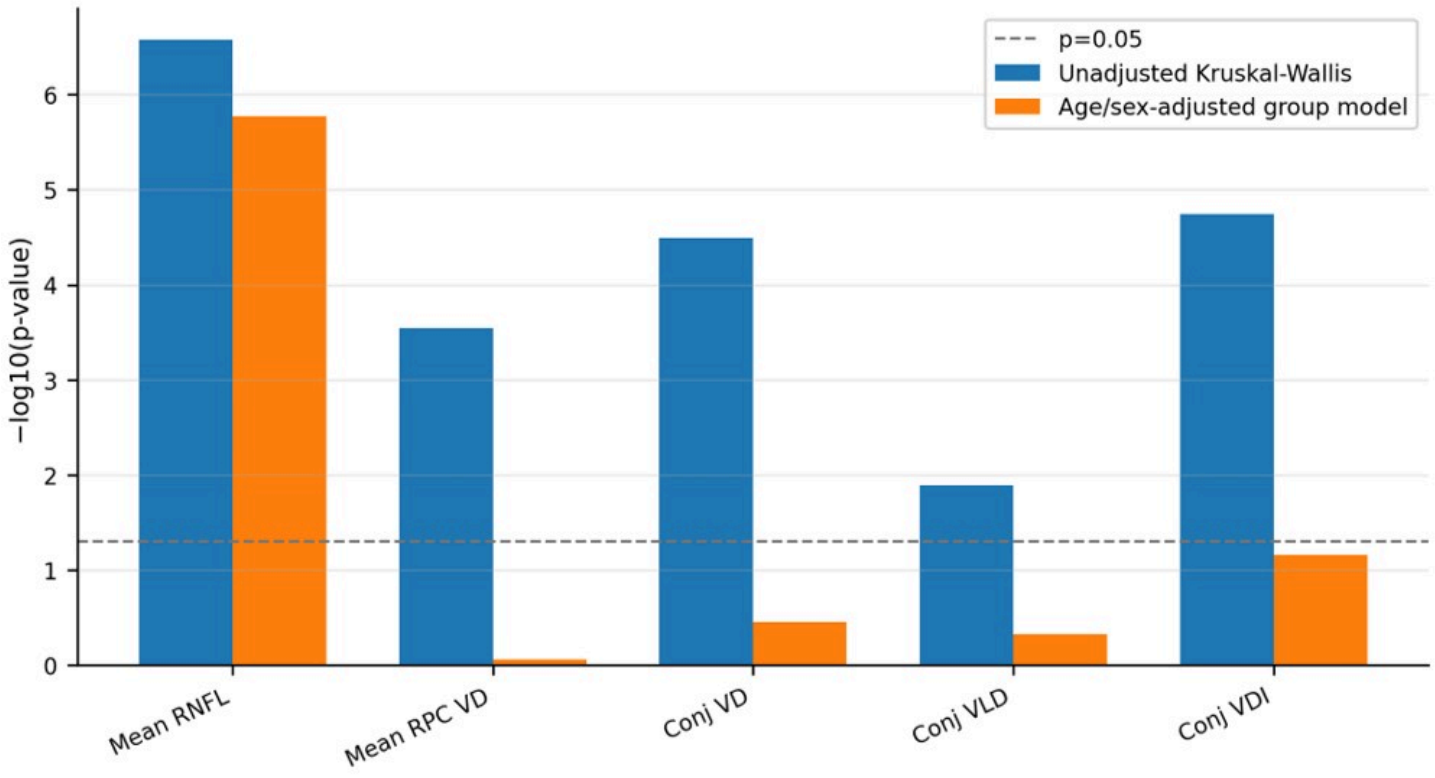


Figure 6

Impact of age/sex adjustment on domain-level inference. Vascular-domain significance attenuates after adjustment, whereas RNFL remains robust.